A ONE-CHIP SCANNING RETINA WITH AN INTEGRATED MICRO-MECHANICAL SCANNING ACTUATOR FOR A COMPOUND EYE VISUAL SENSOR

Kazunori Hoshino, Fabrizio Mura, Isao Shimoyama
Department of Mechano-Informatics, The University of Tokyo
7-3-1, Hongo, Bunkyo-ku, Tokyo 113-8656, Japan
Phone: +81-3-5841-6318, fax: +81-3-3818-0835
E-mail: (hoshino, fabrizio, isao)@leopard.t.u-tokyo.ac.jp

ABSTRACT

A micro-sensor that merges sensing and scanning functions on a single-chip has been designed and fabricated, resulting in the successful design of the first integrated scanning retina of its kind. A micro-fabrication technique has been developed in order to combine a microlens array together with a photo-diode array and an electrostatically driven scanning slit on a single chip. The movement of the electrostatic scanner generates an effect similar to that of "retinal scanning vergence" found in the insects' compound eyes. With the fully integrated silicon scanning retina with a micro mechanical scanner, we propose a new architecture of *Retinal Scanning* which enhances the resolution of a visual sensor.

INTRODUCTION

The insect compound eye is a sophisticated micro visual sensor which has been thoroughly evolved by nature to integrate micro opto-electro-mechanical components within its volume of several mm^3 to take full advantage of scale effects in the world of microsystems. Given the relatively small number of neurons, the fast and robust parallel processing of the insect visual system suggests a highly efficient visual processing circuitry with compact tunable networks

Several studies in robotics have focused on the structure and function of insect vision in order to develop visual sensors for robotic applications [1], [2]. Some studies have also highlighted the integration of "artificial retinas" which consist of photoreceptors and signal processing circuitry on a single chip [11], [14], [17]. These studies are mainly dealing with the neuronal functions of the living animal's visual systems. However, the opto-mechanical structure of the insect compound eye is also an essential part of the processing of visual information at the micro-scale level.

Recent studies in neurobiology have reported on the existence of repetitive retinal movements in insect eyes[3]. It is believed that retinal movements improve the visual system's resolution. Standard MEMS techniques for fabrication of separate elements, such as microlenses[13], [18], micro-actuators, photoreceptors and signal processing circuitry, have been thoroughly investigated. These techniques have been applied to

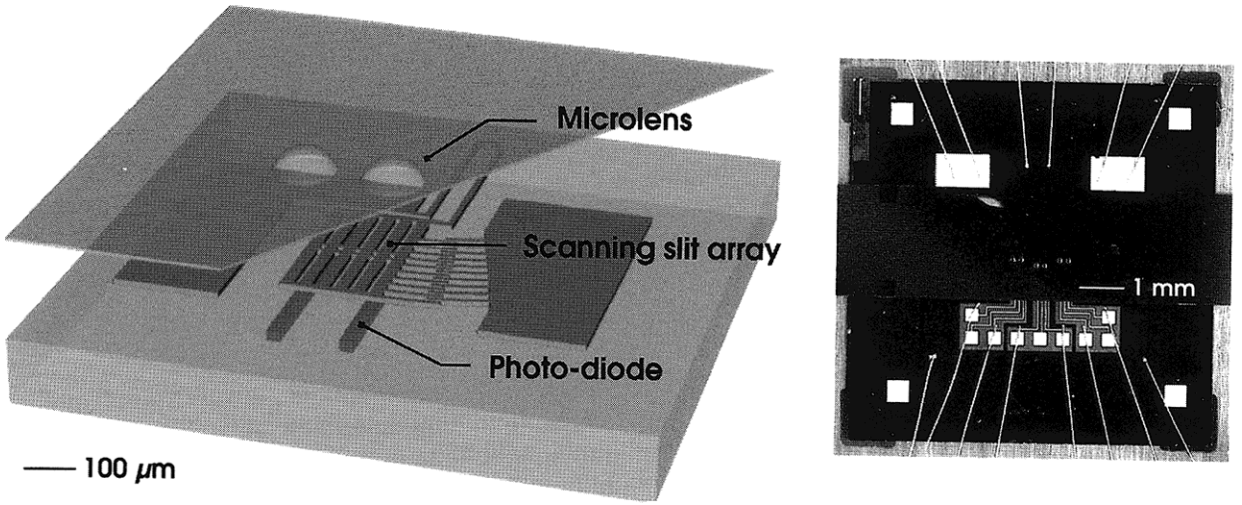

Figure 1. A schematic view (left) and a top view photograph (right) of the scanning visual sensor. A microlens array is aligned and placed over a scanning retina, which comprises an electrostatically driven scanning actuator.

the design of complete micro optical systems, in particular for laser scanning or communicating devices [7], [8], [9]. The technical feasibility of the microcomponents and microsensors has encouraged the fabrication of a scanning visual sensor inspired by the insects' retinal movements. This study is the first approach to construct a smart vision chip equipped with a mechanical scanning component. We propose a new architecture of *Retinal Scanning* which enhances the resolution of a visual sensor with an integrated micro-mechanical scanner and a photo detector array.

The theoretical and experimental effects of retinal scanning in large-sized systems and a micro-sized visual system with a large-sized external actuator were investigated in earlier studies[5], [6], [12]. This paper reports on a newly fabricated micro scanning retina where the scanning slit arrays and a photodiode array are integrated on a single chip. Loaded with a microlens array, this scanning retina generates a rotational movement of the visual axes. The slit array, actuated by a frictionless electrostatic actuator contributes to downsizing the visual system.

DESIGN AND FABRICATION

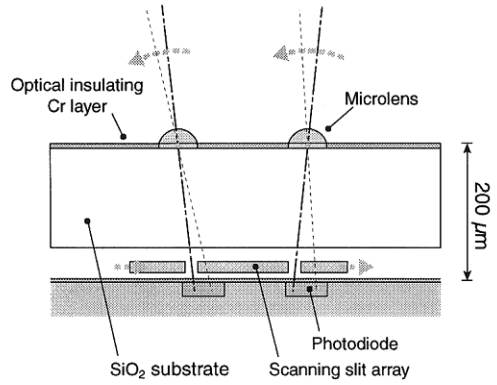

Figure 2. A cross-section showing the structure of the scanning visual sensor. The slits, actuated on top of the photodiodes, change the orientation of the active window with respect to the visual axes.

Figure 1 shows a schematic view of the micro scanning visual sensor. The microlens array, fabricated using melting photoresist technology, is aligned and fixed over the scanning retina. The slits, actuated on top of the photodiodes, change the orientation of the active window with respect to the visual axes (see also figure 2).

Fabrication of the Scanning retina

The scanning retina is composed of a photo-diode array and a mechanical scanning actuator. The photodiodes are made by a thermal ion diffusion process. Boron ions are deposited by spincoating a poly boron film (PBF) onto an N doped silicon substrate and diffused to form P+ regions. The depth of the PN junction measured using the spherical drill method is found to be 1.2μm. The scanning actuator is made of poly-Si and driven by electrostatic force[16]. A slit array actuated by the scanning actuator is fabricated on top the photodiodes.

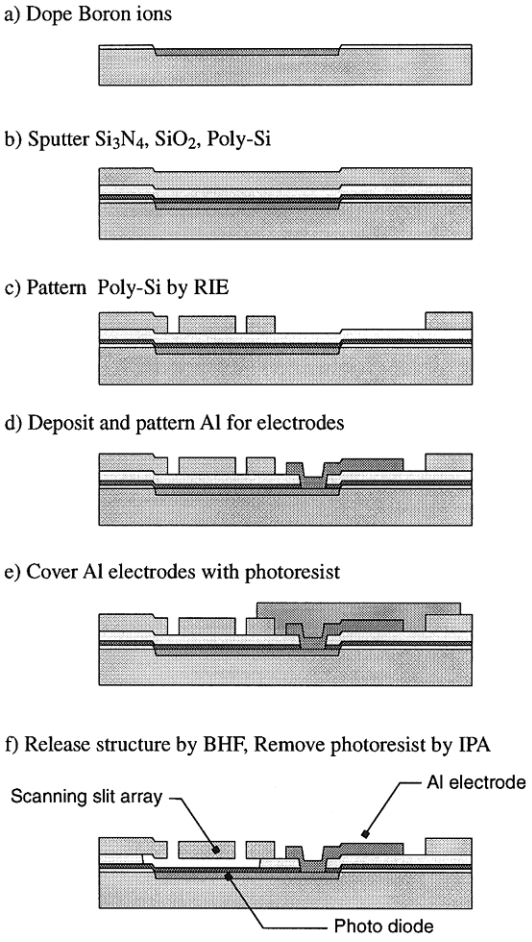

Figure 3. The fabrication process of the scanning retina. b) After insulating the photodiode array with a passivating layer of Si_3N_4, a SiO_2 sacrificial layer and a poly-Si structural layer are then sputtered. e) Al electrodes are covered with a patterned photoresist before the wet etching process to prevent Al from being etched.

Figure 3 shows the fabrication process of the scanning retina. After passivating the photodiodes with a etch-

stop layer of Si_3N_4, a sacrificial layer of 2μm-thick SiO_2 and a structural layer of 4μm-thick P-doped poly-Si are sputtered and stress-annealed at 1100°C for 30 minutes. The scanning actuator's structure is patterned by reactive ion etching using SF_6, O_2 and CHF_3 gas mixture[10]. Contact windows to the photodiodes are opened and an Al layer for electrodes are sputtered and patterned. Before the wet etching process of the sacrificial layer in BHF, the Al electrodes are covered with a patterned photoresist to prevent Al from being etched and the photoresist is removed by IPA after the process.

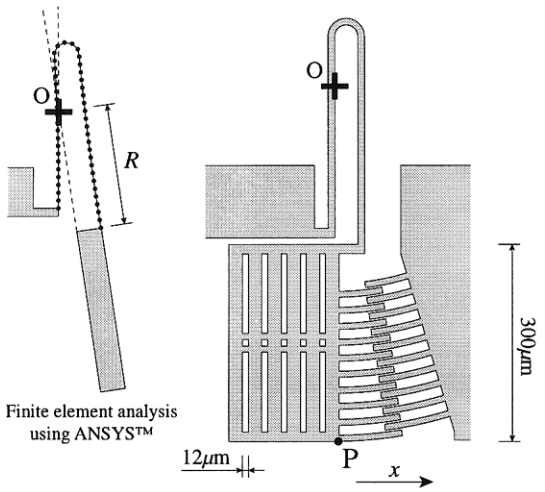

Figure 4. Design of the scanning slit array. From a finite element analysis of the single beam support, point O in the figure can be approximated as the center of the rotation.

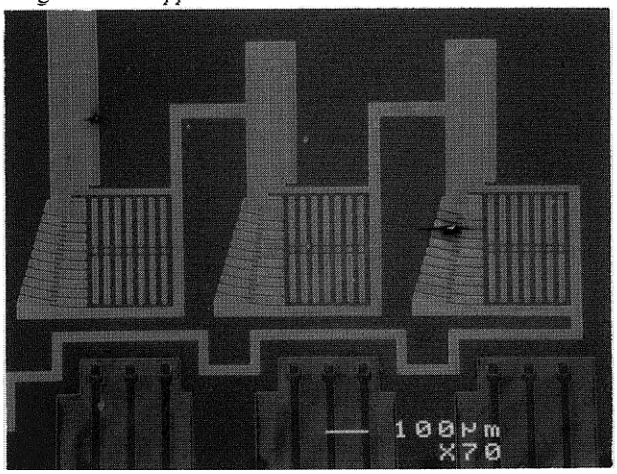

Figure 5. An SEM photograph of three slit arrays fabricated on the scanning retina. Al contacts to the photodiodes are seen in the top of the photograph.

Figure 4 shows the design of the scanning actuator. Supported by a single beam, the scanning slit array can be actuated at a low driving voltage and undergoes a rotation whose center can be approximated at the point O in the figure. In this design, the active surface of the photodiode is 30μm wide and the moving slits is 12μm wide. The scanning displacement Δl is related to the focal distance of the lens f and the scanning angle $\Delta\xi$ in the following way,

$$f\tan(\Delta\xi) = \Delta l \,. \qquad (1)$$

Since the focal distance f of the microlens is very small (200μm) compared to a conventional one-lens system, the required scanning displacement of the slits can be adjusted to match the theoretical requirements of retinal scanning. For example, a displacement of 15μm is required to generate an angular displacement of 4 degrees.

Microlens array

The microlens array is fabricated using the melting patterned photoresist technology[13]. A thick photoresist named Clariant® AZ P4620 is patterned cylindrically on the substrate and melted to compose a microlens.

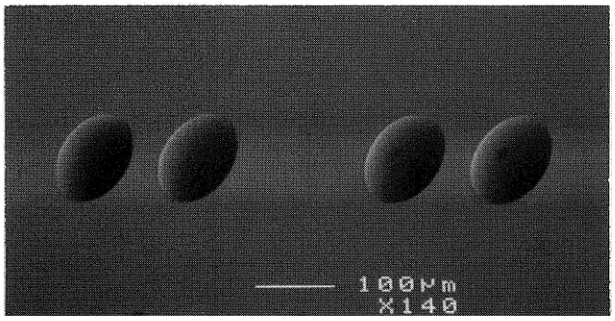

Figure 6. The microlens array fabricated on a SiO_2 substrate using melting photoresist technology. The lenses are 120 μm in diameter.

The focal distance of a melting photoresist lens is given by the following expression[13]

$$f = \frac{h_L + r^2/h_L}{2(n-1)}, \qquad (2)$$

where r, h_L and n represent the radius, the height and the refractive index of the lens ($n \approx 1.5$), respectively. The height of the lens h_L can be adjusted by controlling the thickness of the patterned cylindrical photoresist. In this case, the focal distance of 200μm is obtained with the condition; $r = 60$ μm and $h_L = 18\mu$m. The microlenses are arranged on a SiO_2 substrate of 150μm thickness. Each microlens is optically insulated from the rest of the array by sputtering a thin Cr layer around

the area of lens on the top surface of the SiO_2 substrate.

CHARACTERISTICS

Mechanical response

The mechanical response of the slit array is shown in figure 7. The resonant frequency measured with a strobe microscope is 1200Hz. In a non-resonant mode, the scanner is required to move in the frequency band of 5-20Hz. A sinusoidal wave control voltage of 50Vp-p is sufficient to generate a displacement of the slit array of 20μm.

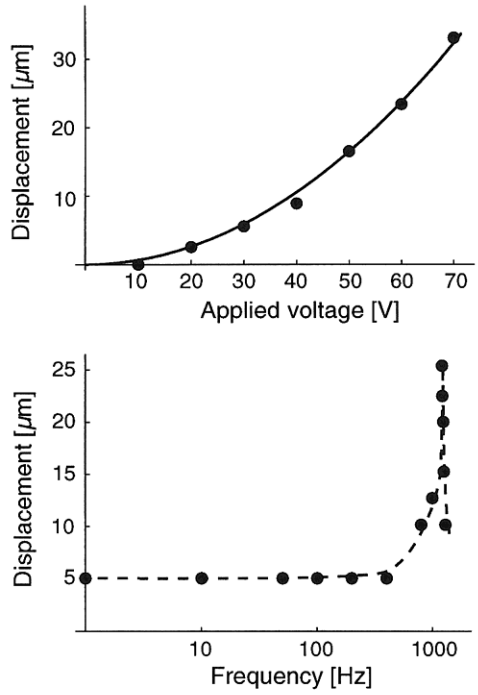

Figure 7. Mechanical response of the scanning actuator. The resonant frequency measures 1200Hz. A control voltage of 50Vp-p is sufficient to generate a designed displacement of 15-20μm at 5-20Hz.

Optical characteristics

In order to estimate the optical characteristics of the visual system, the angular resolution of an individual visual unit is measured. Black and white contrast patterns with several angular frequencies are moved in front of a visual unit taken from the visual sensor and the output modulation of the photo-detector is measured for each angular frequency. In practice, the contrasts are printed on a white board and the luminance of the black and white stripes changes from 100 lux to 1600 lux. As the angular frequency of a pattern increases, the modulation resolved by the visual units gets smaller.

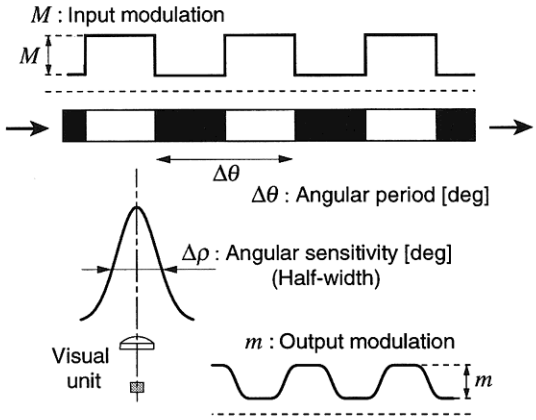

Figure 8. The relative modulation of light intensity induced by movement of a striped pattern is given by the stripes' angular period and the visual unit's angular sensitivity.

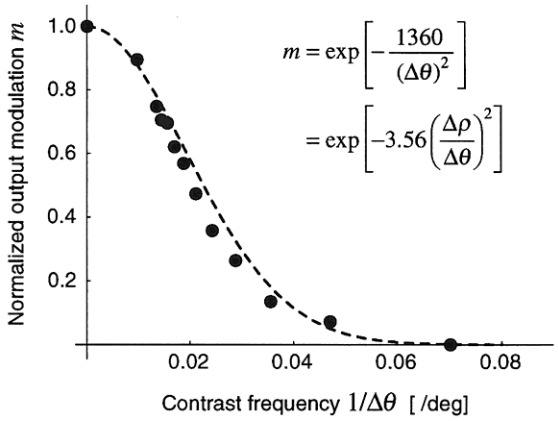

Figure 9. Measured modulation transfer function. The measurement shows a good fit to the principle introduced by [4] and [15]. The angular sensitivity of an individual visual unit is calculated as $\Delta\rho = 20°$.

Fig 9 shows the normalized output modulation of the visual unit, when the contrast of the original stripes is set to 100%. According to [4] and [15], if it is assumed that the shape of the angular receptive field of the visual unit follows Gaussian, the output modulation m is given by

$$m = \exp\left[-3.56\left(\frac{\Delta\rho}{\Delta\theta}\right)^2\right], \qquad (3)$$

where $\Delta\rho$ is the half-width of the angular receptive field and $\Delta\theta$ is the angular field of a contrast pattern as shown in figure 10. On the other hand, the curve fitting of the measured data to $y = e^{-cx^2}$ is given by

$$m = \exp\left[-\frac{1360}{(\Delta\theta)^2}\right]. \quad (4)$$

From the equation (3) and (4), the angular sensitivity $\Delta\rho$ is calculated as

$$\Delta\rho = 20^\circ. \quad (5)$$

RETINAL SCANNING

In order for the visual sensor to detect a contrast, signals from the photodiodes are amplified and band-pass filtered so that the modulation of light intensity due to the sensor's scanning motion is detected in the form of electric pulses. In this case, the amplitude of the electric pulses is proportional to the angular velocity of the scanning motion Ω_r.

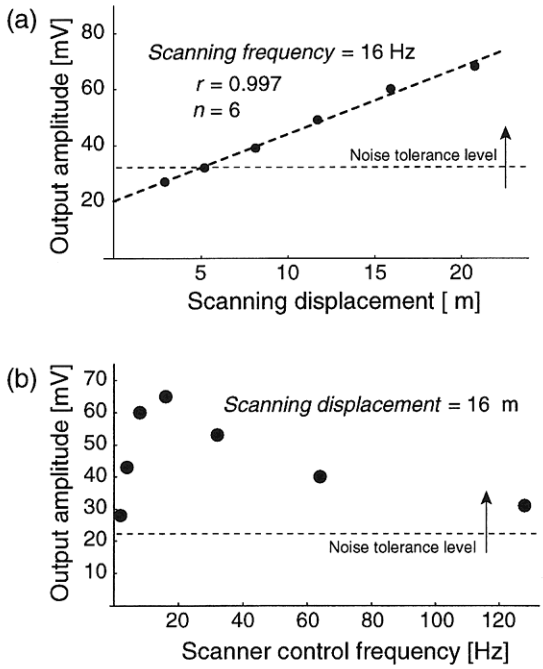

Figure 10. The sensor's output amplitude is measured for several scanning conditions. At a constant scanning frequency, the output amplitude is proportional to the scanning displacement (a). On the other hand, scanning condition of 16 Hz is optimal at the constant scanning displacement due to the band-pass filter's chracteristics (b). With optimized frequency and increased displacement, retinal scanning enhances the output amplitude.

Figure 10 shows the measured relationship of the sensor's output amplitude to the scanning displacement and frequency. At the constant frequency of 16Hz, Ω_r is proportional to the scanning displacement Δl and therefore the output amplitude is also proportional to Δl as shown in figure 10a. On the other hand, at the constant scanning displacement of 16μm, the optimized output amplitude is obtained at the scanning frequency of 16Hz due to the band-pass filter effect and decreases at higher frequencies as shown in figure 10b. The results indicate that with optimized frequency and increased displacement, retinal scanning amplifies the amplitude of the output pulse corresponding to a light contrast within the band-width of the filter circuitry, i.e. retinal scanning increases the S/N ratio of the signals.

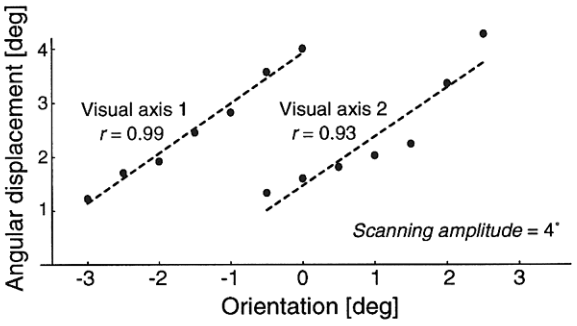

Figure 11. The angular position of a light contrast is measured by two adjacent visual units for every 0.5 degrees.

Figure 11 shows the angular position of a light contrast measured by the visual sensor. The orientation of the light contrast is changed for every 0.5 degrees and the angular displacement with which the contrast is detected by two visual units is measured. The angular displacement can be measured as the phase-shift between the scanner control signal and the output pulse; namely, the angular displacement is measured from the signals in temporal domain to take advantage of the sensors' analogue parallel processing circuitry. The result shows that retinal scanning allows each visual unit to cover a visual field of 3 degrees with an enhanced resolution of 0.5 degrees.

CONCLUSION

A one-chip scanning retina with an integrated micro-mechanical actuator has been designed and fabricated for a micro-sized compound eye visual sensor. The opto-mechanical properties of the visual sensor have been evaluated.

Although the visual units of the sensor without scanning do not have a high spatial resolution, the array of the visual units can detect a contrast with a high temporal resolution. The scanning motion of the retina induces a rotational movement of each visual axis, and therefore the angular position of a light contrast is acquired by the

array of the scanning visual units in temporal domain. The experiment has shown that each visual unit covers a visual field of 3 degrees with the resolution of 0.5 degrees. Furthermore, any number of slit arrays and photodiodes can be easily arranged on a single-chip by a photolithography process. Figure 5 shows a sample of three slit arrays arranged on the scanning retina.

This study is the first successful approach to downsize the scanning visual sensor into the scale of the insects' visual systems. The silicon scanning retina has shown the feasibility to build a totally integrated micro-mechanical artificial visual system.

ACKNOWLEDGEMENT

This research is supported by the PROgram for the promotion of Basic Research Activities for INnovative biosciences (PROBRAIN) under the supervision of the ministry of agriculture and fisheries in Japan. K. Hoshino is supported by the Japan Society for the Promotion of Science (JSPS). F. Mura received a joint EU-JSPS post-doctoral fellowship for this research.

REFERENCES

[1] J.S. Charl, M.V. Srinivasan, "Range Estimation with a Panoramic Visual Sensor," Journal of Optical Society of America 14, pp. 2144-2151, 1997.

[2] N. Franceschini, J.M. Pichon, C. Blanes, "From Insect Vision to Robot Vision," Phil. Trans. R. Soc. Lond. B, 337, 283-294, 1992.

[3] N. Franceschini, R. Chagneux, "Repetitive Scanning in the Fly Compound Eye," Proc. 25th Göttingen Neurobiology Conference eds Elsner & Wässle, p. 279, 1997.

[4] G.A. Horridge, "The Separation of Visual Axes in Apposition Compound Eyes," Phil Trans R Soc Lond B, 285, pp. 1-59, 1978.

[5] K. Hoshino, F. Mura, H. Morii, K. Suematsu, I. Shimoyama, "A Small-Sized Panoramic Visual Sensor Inspired by the Fly's Compound Eye," Proc. IEEE ICRA '98, Leuven, Belgium, pp. 1641-1646, 1998.

[6] K. Hoshino, F. Mura, I Shimoyama, "A Micro-Sized Visual Sensor Based on the Fly's Eye with a Scanning Retina," Proc. IEEE MEMS, Orlando, Florida, pp.429-434, 1999.

[7] M. Ikeda, H. totani, A. Akiba, H. Goto, M. Matsumoto, T. Yada, "PZT Thin-Film Actuator Driven Micro Optical Scanning Sensor by 3D integration of Optical and Mechanical Devices," Proc IEEE MEMS, Orlando, Florida, pp.435-440, 1999.

[8] M.H. Kiang, O. Solgaard, R.S. Muller, K.Y. Lau, "Surface-Micromachined Electrostatic-Comb Driven Scanning Micromirrors for Barcode Scanners," Proc. IEEE MEMS, pp. 192-197, 1996.

[9] M Kobayashi, H. Toshiyoshi, H. Fujita, "A Micromechanical Tunable Interferometer for Free-Space Optical Interconnection," Proc. IEEE/LEOS MOEMS'97, Nara, pp. 171-175, 1997.

[10] R. Legtenberg, H. Jansen, M. Boer, M. Elwenspoek, "Anisotropic Reactive Ion Etching of Silicon Using $SF_6/O_2/CHF_3$ Gas Mixtures," Journal of Electrochemical Society, vol. 142, No. 6, pp. 2020-2028, 1995

[11] C. Mead, "Analog VLSI and Neural Systems," Addison Wesley, Reading, MA, 1989.

[12] F. Mura, N. Franceschini, "Obstacle Avoidance in a Terrestrial Mobile Robot Provided With a Scanning Retina," Proc. IEEE Intelligent Vehicles Symposium, Tokyo, pp, 47-52, 1996.

[13] Ph. Nussbaum, R. Völkel, H. P. Hertzig, R Dändliker, "Microoptics for Sensor Applications, " Proc. European Symp. Lasers, Optics and Vision for Productivity in Manufacturing, 2783, pp. 1-9, 1996.

[14] P. Questa, G. Sandini, "Time to Contact Computation with a Space-Variant Retina-like C-MOS Sensor," Proc. IROS 96, pp. 1622-1629, 1996.

[15] A. W. Snyder, "The Physics of Vision in Compound eyes," Handbook of Sensory Physiology, ed Autrum, vol VII/6, Springer Verlag, Berlin & New York, pp 215-313, 1979.

[16] W.C. Tang, T.H. Nguyen, R.T. Howe, "Laterally Driven Polysilicon Resonant Microstructures," Proc. MEMS, pp. 53-59, 1989.

[17] E. Lange, Y. Nitta, K. Kyuma, "Optical Neural Chips, " IEEE MICRO, vol 14, #6, pp. 29-41, 1994.

[18] Y. Xia, E. Kim, X.M. Zhao, J. A. Rogers, M. Prentiss, G. M. Whitesides, "Complex Optical Surfaces Formed by Replica Molding Against Elastomeric Masters, " Science, vol. 273, pp. 347-349, 1996.